European Review for Medical and Pharmacological Sciences 2021; 25: 3997-4004

Screening and characterization of aptamers for recombinant human programmed death-1 and recombinant extracellular domain of human programmed death ligand-1

Z.-F. LI[1,2], C. CHEN[2], J.-Y. ZENG[2], S. WANG[2], S.-Q. HAN[1], Y.-Q. ZHANG[1], D.-D. QIU[2], H.-X. GUO[2]

[1]School of Medicine, Huaqiao University, Fujian, China
[2]Institute of Molecular Medicine, Huaqiao University, Fujian, China

Abstract. – OBJECTIVE: Programmed death ligand-1 (PD-L1) is expressed on tumor cells and macrophages. The detection of PD-L1 expression in cancer and the treatment by targeting the PD-L1/programmed death-1 (PD-1) are of great clinical significance. This work aims to screen the aptamers with high affinity and specificity for recombinant human PD-1 (rhPD-1)/recombinant human PD-L1 extracellular domain (rhPD-L1).

MATERIALS AND METHODS: In this study, we have expressed, purified, prepared, and identified rhPD-1 and rhPD-L1. The rhPD-L1/rhPD-1 aptamers with high affinity and specificity were obtained by systematic evolution of ligands by exponential enrichment technique. Ten aptamers sequences to rhPD-L1 and 10 aptamers sequences to rhPD-1 were obtained by cloning and sequencing. The affinity and specificity of candidate aptamers were analyzed by gold nanoparticles-based colorimetric assay, dot blot assay, and electrophoretic mobility shift assay.

RESULTS: The aptamers named A6 were picked out as the optimal aptamers that recognize PD-1, specifically with the Kd value of 47.84 ± 24.78 nM. The aptamers named B10 were picked out as the optimal aptamers that recognize PD-L1, specifically with the Kd value of 59.72 ± 15.87 nM.

CONCLUSIONS: The study lays a foundation for the development of detection methods and therapeutic drugs targeting PD-L1/PD-1.

Key Words:
Programmed death-1, Programmed death ligand-1, Systematic evolution of ligands by exponential enrichment, Dot blot, Electrophoretic mobility shift, Gold nanoparticles.

Introduction

The immune system participates in recognizing self/non-self and inhibiting the development of diseases with both endogenous and exogenous origins by this means[1,2]. Cancer cells avoid immune surveillance by overexpressing negative immunologic regulators[3]. PD-1 is an inhibitory receptor, mainly expressed on activated T cells, certain B cells, natural killer cells, dendritic cells, and macrophages, and leads to apoptosis[4-6]. PD-L1 is expressed on inflammatory-activated immune cells, including macrophages, T cells, B cells, keratinocytes, endothelial and intestinal epithelial cells, as well as a variety of carcinomas and melanoma[7,8]. PD-1/PD-L1 participates in the proliferation and secretion of T cells that are involved in the suppression of antitumor immune reactions[1,8]. It was demonstrated that by suppressing PD-1/PD-L1, a great increase occurs in cancer immunotherapy, and the progression and development of cancer undergo inhibition[9].

Aptamers are single-stranded DNA (ssDNA) or RNA selected and prepared by systematic evolution of ligands by exponential enrichment (SELEX) that are able to bind specifically to target molecules with high affinity[10,11]. Aptamers exhibit competitive advantages over other natural or artificial receptors, such as synthesis convenience, tight-binding capability, chemical stability, and flexibility of chemical modification for labeling or favor immobilization[11]. The unique properties of nucleic acids endow aptamers with lots of relative advantages to antibodies, including nonimmune, low-cost, fast time preparation, and thermal stability. Hence, they are widely applied in various detection applications[12]. Aptamers are also of smaller size compared to antibodies, leading to faster and more internalization of aptamers into tumors.

Corresponding Author: Zhaofa Li, Ph.D; e-mail: lizhaofa@hqu.edu.cn

Because of these excellent properties, aptamers have growing wider applications in cancer treatment and diagnosis[13,14].

In this article, we describe the selection of aptamers sequences for rhPD-1 and rhPD-L1 by SELEX. With this universal technology, novel aptamers specific to target molecules are rapidly identified and selected. Gold nanoparticles (AuNPs)-based colorimetric assay, dot blot assay, and electrophoretic mobility shift assay (EMSA) were used to identify the binding properties of the selected aptamers toward rhPD-1 and rhPD-L1.

Materials and Methods

Apparatus and Reagents

Apparatus: Tanon-4600SF full-automatic chemiluminescence gel imaging analyzer (Shanghai Tianneng Technology Co., LTD, Shanghai, China), Bioshine gel imaging (Shanghai Ouxiang Scientific Instrument Co., LTD, Shanghai, China).

Reagents: All the DNAs used in this study were synthesized commercially by Thermo Fisher Scientific company, Shanghai, China.

Cloning, Expression, and Purification

The proteins of rhPD-1 and rhPD-L1 were cloned, expressed, and purified as described earlier[3,15]. The gene encoding human PD-L1 (amino acids 18-134) and human PD-1 (33-150, Cys93 exchanged to serine) was cloned into pET-22b. Proteins were expressed in *Escherichia coli* BL21 (DE3). Cells were cultured in LB at 37°C. The protein production was induced with 1 mM IPTG at OD600 of 1.0, and the cells were cultured for additional 4 h. For rhPD-1 and rhPD-L1, the temperature dropped to 30°C after induction. The protein was expressed as inclusion bodies, collected by centrifugation, washed twice with 50 mM Tris-HCl pH 8.0 containing 500 mM NaCl, 0.5% Triton X-100, 10 mM EDTA, and 8M urea, and washed once again with the same buffer. The inclusion bodies were dissolved in 50 mM Tris pH 8.0 containing 2M urea, 500 mM NaCl, and 10 mM EDTA overnight. They were frozen and centrifuged at high speed to obtain the dissolved supernatant and filtered with a 0.45 μm filter membrane. rhPD-1 and rhPD-L1were desalted with Sephadex G-25 column and refolded into 20 mmol/L Tris-HCl (pH 8.0). Using a tangential flow ultrafiltration concentration device and a 3-kDa molecular weight cutoff membrane pore size, the protein was ultrafiltration concentrated and purified by Sephacryl S-100 size exclusion chromatography in 20 mM Tris pH 8.0 containing 0.5 M NaCl. The purified proteins were evaluated by tricine-SDS-PAGE, Western blot, and peptide mass fingerprint analysis.

Tricine-SDS-PAGE, Western Blot, and Analysis of Peptide Mass Fingerprinting

Tricine-SDS-PAGE was conducted according to the method by Schägger[16]. Tricine-SDS-PAGE proteins were resolved on polyacrylamide gels (60×80×1 mm). Use 4% concentrated gel, and 16.5% separation gel, with 30:1 acrylamide:bisacrylamide ratio. Twenty millimolar Tris-HCl, 10 mM Tricine, 0.1% (w/v) SDS 1 x cathode buffer (pH 8.3) was added to the electrophoresis tank, and 50 mM Tris 1 x anode buffer (pH 8.9) was added to the electrophoresis tank. The vertical electrophoresis device was placed in ice, and the gel and interlayer gel were concentrated. The electrophoresis was at a constant voltage of 30V for 1 h, and the separation gel was adjusted to 100V until the bromophenol blue indicator reaches the bottom of the gel to terminate the electrophoresis. The glass plate was removed, and the gel was taken out. The protein gel was immersed in 200 mL of fixative solution and shaken at room temperature.

The Western blot was used for the examination of rhPD-1 and rhPD-L1 to confirm the tricine-SDS-PAGE results. After tricine-SDS-PAGE, the prestained protein standards were used to compare and confirm the position of the target protein band, and the target fragment was cut out and transferred from the gel to a polyvinylidene fluoride (PVDF) membrane (Bio-Rad, Hercules, CA, USA). The membrane was blocked with 2% skimmed milk powder (containing 0.2% Tween-20) for 1 h. The primary antibody was used at a dilution of 1:1000 in Tris-Buffered Saline and Tween (TBST) and incubated overnight at 4°C. Anti-rabbit IgG was used as the secondary antibody, diluted with TBST at a ratio of 1:2000, and incubated at room temperature for 1 to 2 h. After the incubation is over, the gel was washed three times with TBST and ECL developer was added. The blots were exposed using Tanon-4600SF full-automatic chemiluminescence gel imaging analyzer.

The purified product to be identified was separated by tricine-SDS-PAGE electrophoresis, stained, and decolorized, and the target fragment was compared with the prestained standard

molecular weight protein Marker. The correct protein fragment of interest was cut, placed in a clean and sterile 1.5 mL EP tube, and the sample was sent to Shanghai Sangon Biotech Co., Ltd. for analyzing peptide mass fingerprinting.

In Vitro Selection

The sequences of random library and primers used were as follows: 80 nt (76-mer) random ssDNA library: 5′-AGCAGCACAGAGGTCAGATG-N40-CCTATGCGTGCTACCGTGAA -3′), forward primer: 5'-GATACTGCGTGCTTGTTCCATA-3', and amino-modified reverse primers: 5'-NH2-C6-GGCAACTTCTCACTTACTGTCA-3'.

For the aptamers selection process, rhPD-1 protein and rhPD-L1protein (0.5 mg/mL) were fixed with activated 25 µL amino magnetic beads (10 mg/mL) 3 h, respectively. It was fixed with ssDNA primary aptamers library (6 µM) for 2 h blocking with 1% BSA for 1 h. Then, the supernatant containing target-bound sequences was collected using magnetic separation for polymerase chain reaction (PCR) amplification. Five hundred–microliter PCR amplification was made of 50 µL ssDNA template, 10 µL forward primer (4 µM), 10 µL reverse primer (4 µM), 3 µL rTaq DNA polymerase (5 U), 4 µL dNTP (2.5 nM), 50 µL10xPCR buffer, and 373 µL ultrapure water. The PCR reaction was performed as follows: Predenaturation was done at 95°C for 10 minutes, and denaturation was done at 95°C for 30 s. Annealing was done at 60°C for 30 s, whereas extension was done at 72°C for 30 s, and re-extension was done at 72°C for 10 minutes. It was cooled at 4°C. Polyacrylamide gel electrophoresis was used to identify PCR products. After staining with Gelred, the gel was photographed under UV light to confirm 80 bp size of PCR products.

The enriched aptamers product was identified and recovered by 8% polyacrylamide gel electrophoresis. The concentration of the purified PCR product was quantified using a NanoDrop 3300 fluorescence spectrophotometer. Real-time fluorescence quantitative PCR (qPCR) was used to determine its expansion intensity. Two hundred microliter qPCR amplification was made of 20 µL ssDNA template, 4 µL forward primer (1 µM), 4 µL reverse primer (1 µM), 2.4 µL rTaq DNA polymerase (5U), 1.6 µL dNTP (2.5 nM), 20 µL EvaGreen (20x), 20 µL10xPCR buffer and 138 µL ultrapure water. The qPCR reaction was performed as follows: Predenaturation was done at 95°C for 5 minutes. Denaturation was done at 95°C for 30 s. Annealing was done at 60°C for 30 s, whereas extension was done at 72°C for 30 s. The conditions of qPCR melting curve were as follows: 95°C, 15s. 60°C, 60s. 95°C, 15s. 45°C, 5 s. The generated ssDNA was stored in 1xTE buffer or used in the next round of SELEX selection.

Cloned and Sequencing

After 13 rounds of SELEX selection, the aptamers binding with rhPD-1 protein and rhPD-L1 were enriched, and the PCR products were cloned and sequenced by Shanghai Sunny Biotechnology Co., Ltd. (Shanghai, China).

Identification of Affinity and Specificity

AuNPs, dot blot assay, and EMSA method were used to assess the affinity and specificity of the aptamer's candidates to the PD-1 and PD-L1.

AuNPs were prepared by reducing chloroauric acid with sodium citrate. The binding assays were performed by incubating a series concentration of AuNPs aptamers ranging from 10 to 1000 nM with rhPD-1 protein and rhPD-L1 protein targets (1 mM) at 37°C for 1 h in 300 mL of binding buffer in the dark. Twenty-microliter NaCl (1.2 M) was added and mixed for 0.5 h in the dark. The UV absorption curve was obtained by scanning the full wavelength of UV, and the UV-Vis (detection wavelength 400 nm to 800 nm) was detected. Then, by calculating the ratio of A650/A520 at different aptamers concentrations, the secondary structures of sequences were analyzed by the mfold program.

One microliter target protein (10 µg) was spotted onto the surface of the nitrocellulose membrane (0.22 µm). Once the film dried, it was immersed in 1% BSA solution to block at room temperature for 1.5 h. The excess blocking agent was removed by rinsing with Binding & Washing (B&W) buffer (10 mM Tris-HCl, pH 7.5, 1 mM EDTA, 0.5 M NaCl). The well-blocked membrane was then incubated with aptamers for 2 h. After washing with B&W washing buffer, 1 µL Streptavidin-labeled Horseradish peroxidase was added, diluted with deionized water to 1 mL, incubated in a shaking table for 1 h, and ECL developer was added. The blots were exposed using Tanon-4600SF full-automatic chemiluminescence gel imaging analyzer.

The separated gel was composed of 3.5% polyacrylamide. To speed polymerization, the gel mixture (50 mL) was heated in a microwave oven for 30 s, and then 1% ammonium peroxy-

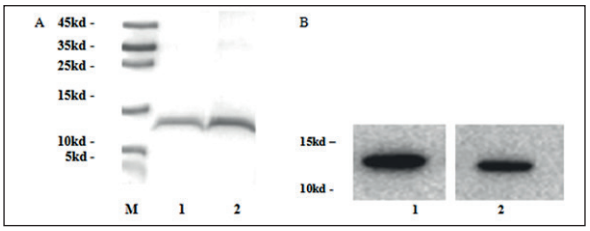

Figure 1. Tricine–SDS-PAGE **(A)** and western blot **(B)** of rhPD-1 and rhPD-L1. M: Protein Marker, 1: Purified rhPD-1, 2: Purified rhPD-L1.

disulfate and N,N,N',N'-tetramethylethylenediamine were added to polymerize the gel (300 V, 180 mA pre-electrophoresis for 10 min). The target protein and ssDNA aptamers were suspended in binding buffer (100 mM NaCl, 100 mM $NaH_2PO_4 \cdot 12H_2O$, 20 mM KH_2PO_4, 10 mM $MgCl_2$, 2.5 mM KCl, pH 7.3) and incubated at room temperature for 1 h. The incubation sample was mixed with 6 x DNA loading buffer, and a set of single ssDNA aptamers (without any incubation treatment) as a control was prepared, and the sample was loaded. After electrophoresis, this was stained at room temperature for 10 min. Using gel imaging system analysis, it was determined whether there is binding phenomenon based on DNA hysteresis.

Results

Tricine-SDS-PAGE and Western Blot

rhPD-1 and rhPD-L1 were detected by tricine-SDS-PAGE electrophoresis. The single protein bands appeared at about 13.7 KDA (rPD-1 protein) and 13.5 KDA (rPD-L1 protein), shown in Figure 1A. The rest of the swim lanes were clean and clear. This indicated that the protein obtained had reached electrophoresis purity.

The purified proteins of rhPD-1 and rhD-L1 were determined by Western blot. The rhPD-1 and rhD-L1 were separated by tricine–SDS-PAGE and transferred to PVDF membrane. XP Rabbit mAb was used as the first antibody of rh-PD-1 and rhD-L1, and anti-Rabbit IgG was used as the second antibody. The rhPD-1 and rhD-L1 bands can be clearly seen in Figure 1B. However, the heterologous control protein has no specific antibody to rhPD-1 and rhD-L1. The purified proteins of rhPD-1 and rhD-L1were confirmed to be of high purity.

Peptide Mass Fingerprinting

The peptide mass fingerprinting of rhPD-1 and rhPD-L1 was evaluated and analyzed using the protein retrieval program (Mascot, SwissProt) based on the initial data provided by Shanghai Shengong Biotechnology Co. The rhPD-1 protein score was 97, and the PD-L1 protein score was 110 (Figure 2A and 2B). According to the principle of score evaluation, the protein had obvious significance when the score was more than 53. In general, the out-of-shadow portion is the matching peptide with significant differences. The rhPD-1 and rh-PD-L1proteins were identified.

In Vitro Selection of Aptamers Against rhPD-1and rhPD-L1

After each round of SELEX, the absorbance of ssDNA was measured by a micro-nucleic acid analyzer, and the data were collected to analyze whether the secondary library was saturated or not. Results are as shown in Figure 3. The affinity between aptamers and their respective target proteins increased gradually with the increase of

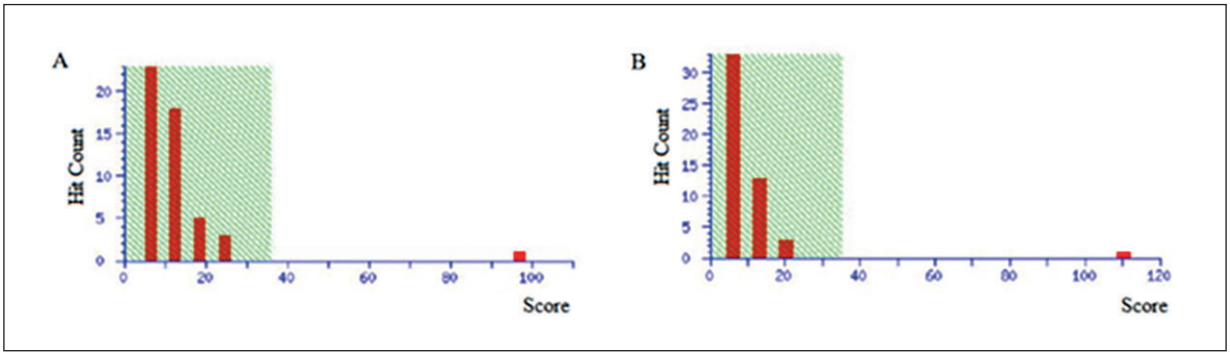

Figure 2. Mascot Score Histogram of rhPD-1 **(A)** and rhPD-L1 **(B)**.

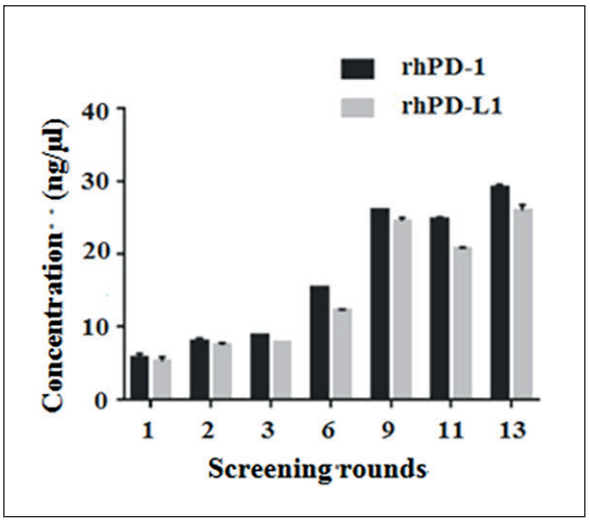

Figure 3. The concentration ratio (PCR products concentration of bound ssDNA/blank control).

screening rounds, and then saturated gradually after nine rounds of enrichment. The screening conditions, such as increasing the concentration of eluted salt and decreasing the PCR system, were further strict in the ninth round. Finally, the SELEX screening was stopped in the 13th round. Twenty candidate sequences to rhPD-1 and rhPD-L1 were obtained by cloning and sequencing.

Binding Affinity and Specificity

The two candidate aptamers sequences (A6 in Table I, B10 in Table II) were chosen by AuNPs-based colorimetric assay (Figures 4A and 5A). The predicted secondary structure of aptamers A6 and b10 are shown in Figures 4B and 5B.

To further evaluate their binding affinity, dot blot assay and EMSA method were introduced.

A6 and B10 were identified by dot hybridization at 300 mM salt concentration. Characterization of the sample system: 100 pmol aptamers, 10 μg target protein. Results (as shown in Figure 6) show that A6 binds to rhPD-1 but not with rhPD-L1 and B10 binds to rhPD-L1but not with rhPD-1. It is suggested that A6 has high affinity and specificity to rhPD-1 and B10 has high affinity and specificity to rhPD-L1.

The concentration of 100 pmol aptamers and 25 μg target protein was determined by EMSA after incubation at room temperature for 2 h. Results are as shown in Figure 7; swim lanes 1

Table I. Sequence (5′-3′) and dissociation constants Kd values of aptamers candidates to PD-1.

Aptamers	Sequences	Kd (nM)
A1	CTTGTGGTCGGCTCGACGCAATACGCTCATACAACGTGGG	344.8 ± 75.378
A2	GGGAGACCATGCTTCGTGCGTCACACTTTGTGAAGCCCTT	Very weak binding
A3	GCACCGGCCAACCGTATGTCTCCCTACAATCTACTGGGAT	Very weak binding
A4	AATAGCCTCACCGCATCATAACCAACCGGTACGCCGAGCG	Very weak binding
A5	TGGCCGACTACCACTATTGCTGCGAATTGGAAAGTGCACA	Very weak binding
A6	ACCGACAGTGAAGGACTCAGCGAACTCTCAGACTCGGTTC	47.84 ± 24.78
A7	CATCGGGTCCAGTGACCTCGGGTCCAGTCTGTGACTAACG	Very weak binding
A8	CGCTTGCGAACAAATACTCTTCCTTTGAAGCCGGACGAC	Very weak binding
A9	TGTCGATAACGAGACATTCTGGCGGACAATATCTGTGACC	Very weak binding
A10	GTACAATATGCGATCCAAATTGGTCTGGACGCGAATTGGC	Very weak binding

Table II. Sequence (5′-3′) and dissociation constants Kd values of aptamers candidates to PD-L1.

Aptamers	Sequences	Kd (nM)
B1	CCAATCGTGGAGATGCCGCCAGTACGCGTTGTACTGTTCG	Very weak binding
B2	CAGAATAGCGTACAGCGACGGAAGGTGCTGCACATAGGGA	Very weak binding
B3	GTATATGATGACAATATACCGTACCGCATAATGCTGATCG	Very weak binding
B4	CGTCCGACGATACCTCCACTCTGTGATCCGCTCCTTGGCG	544.3 ± 85.332
B5	TCGCACATTAGGTAGTGTGGTCGCCGGTAGCCCGGTCCCA	Very weak binding
B6	TGTCTATACCGCCGTAACCGGCTCCTTGAAACCAAGTGGC	Very weak binding
B7	GACCACCTGCACCAATGTGCCAAGGATATGAGCAGTCGAC	Very weak binding
B8	CGAACGAGAAGACTTTTGCCGTCTTCCCTAACCTAGACAC	Very weak binding
B9	GTAGTGCCATGGAACTACTAGTTAGTAGTGCTCACGTCAA	Very weak binding
B10	AACAACGTATAACAATGCCCACGTCACCAGAGTACTATGG	59.72 ± 15.87

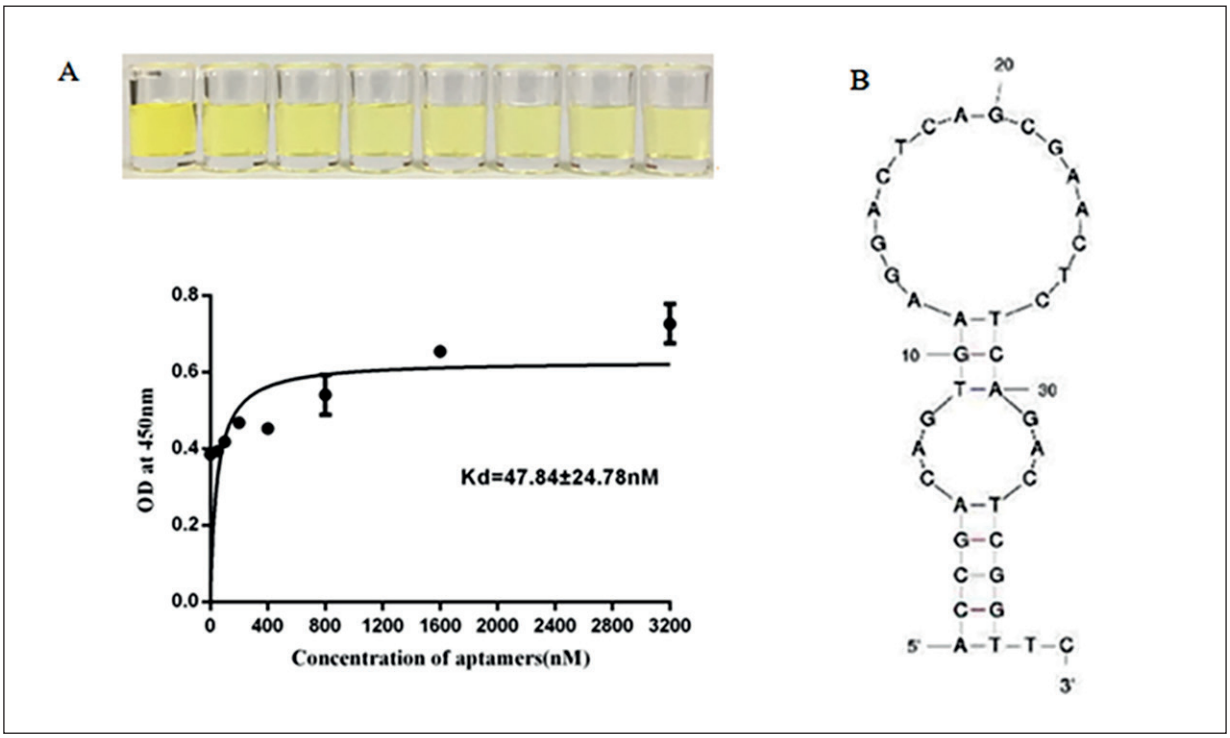

Figure 4. AuNPs-based Colorimetric Assay and secondary structure of A6.

and 3 shift upward, and swim lanes 2 and 4 lag behind. A6 binds to rPD-1 protein to form a macromolecular complex but not with rPD-L1; B10 binds to rPD-L1 protein to form a macromolecular complex but not with rPD-1. Protein–DNA complexes formed on linear DNA fragments result in the characteristic retarded mobility in the gel. It is suggested that A6 has high affinity and

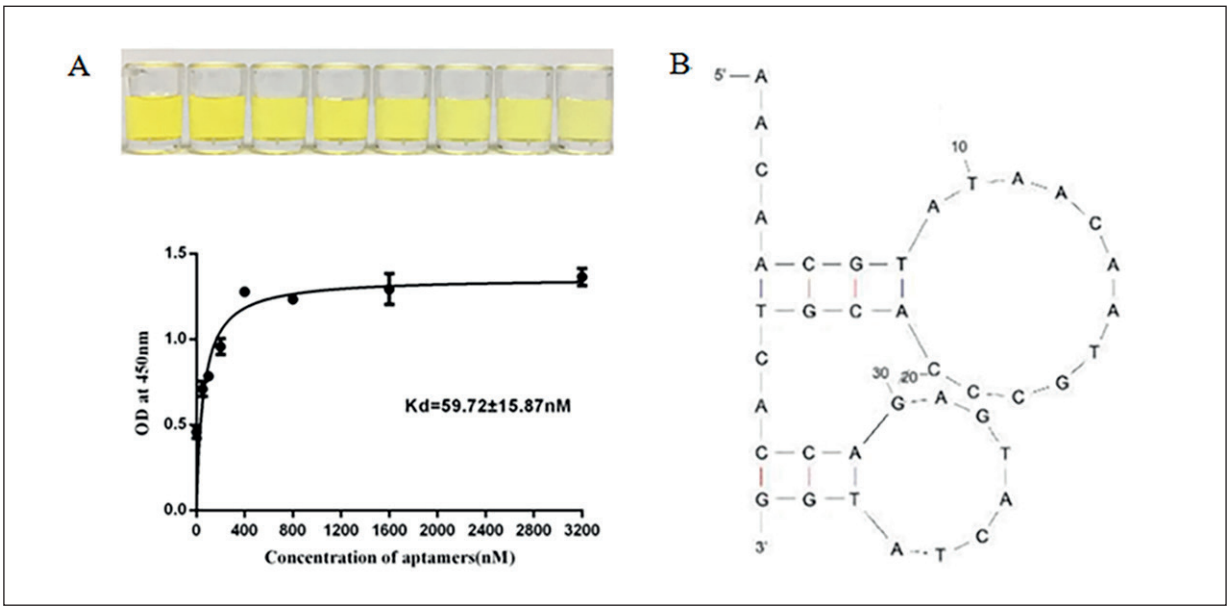

Figure 5. AuNPs-based Colorimetric Assay and the secondary structure of B10.

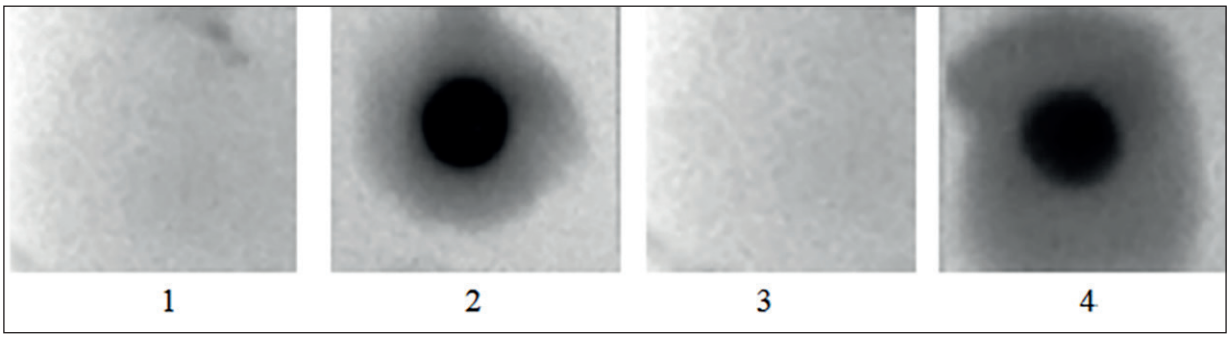

Figure 6. Dot blot assay results of A6 and B10. **1:** A6 negative control (rhPD-L1+A6), **2:** A6 positive (rhPD-1+A6), **3:** B10 negative control (rhPD-1+B10), **4:** B10 positive(rhPD-L1+B10).

specificity to rhPD-1 and B10 has high affinity and specificity to rhPD-L1.

Discussion

Under normal conditions, the pathway prevents excessive stimulation and maintains immune tolerance to self-antigens by negatively regulating the immune response. Conversely, PD-L1 is overexpressed in various tumors, resulting in impaired immune function in the tumor microenvironment. The inhibitors of the PD-1/PD-L1 causing PD-L1 dimerization and PD-1/PD-L1 complex dissociation show effective antitumor activity and rejuvenation of exhausted T-cell phenotypes and cytotoxic functions[17]. Pembrolizumab, the humanized IgG4 monoclonal antibody, has a high affinity with PD-1 and prevents PD-1 interactions with PD-L1 and PD-L2. Avelumab, durvalumab, atezolizumab, envafolimab, and high-affinity human IgG1 promote T-cell activity against the cancerous cells by restricting the binding between PD-L1 and its receptors, PD-1 and B7, overall reversing T-cell suppression[18].

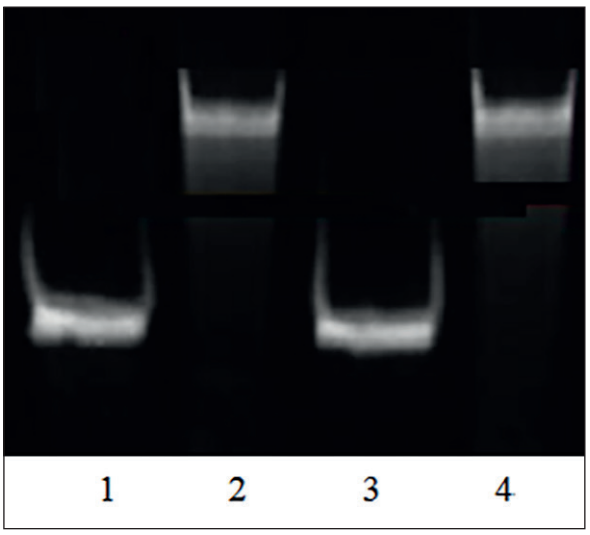

Figure 7. EMSA results of A6 and B10. **1:** A6 negative control (rhPD-L1+A6), **2:** A6 positive (rhPD-1+A6), **3:** B10 negative control (rhPD-1+B10), **4:** B10 positive(rhPD-L1+B10).

Aptamer is a short single-stranded DNA (ssDNA) or RNA sequence selected by systematic evolution of ligands by exponential enrichment (SELEX). Due to folding distinct tertiary structures, aptamers can bind to the corresponding target with high affinity and specificity. Moreover, aptamers also possess several significant advantages, including simple synthesis and modification, high stability, and low immunogenesis[19]. In comparison with traditional antibodies, aptamers are nontoxic, very stable at a vast range of pH, temperature, and ionic environment and can be easily modified with various tags and possess lower immunogenicity and long half-life. Moreover, aptamers are smaller in size compared with antibodies, leading to faster and more internalization of aptamers into tumors. Because of these excellent properties, applications of aptamers are growing quickly in both treatment and diagnosis of cancers[20].

It is because of the significance of PD-1/PD-L1 in tumor detection and treatment and the advantages of aptamers, we cloned, expressed, and purified the proteins of rhPD-1 and rhPD-L1 and screened aptamers of rhPD-1 and rhPD-L1. In the future, the screened aptamers of PD-1/PD-L1applications will be used in the diagnosis and treatment of tumors.

Conclusions

This study uses the SELEX technique to screen aptamers with high affinity and specificity for rhPD-1/rhPD-L1. Among the aptamers candidates, A6 for rhPD-1 and B6 for rhPD-1were identified as the optimal aptamers to probe with the lowest dissociation constant Kd of 47.84 ± 24.78 nM and 59.72 ± 15.87 nM, respectively. In addition, aptamers A6 and B10 were used in dot blot and EMSA for affinity and specificity determination, demonstrating that the selected aptamers have high affinity and specificity from rhPD-1 and rhPD-L1, respectively. Aptamers provide a synthetic alternative to antibodies for research, diagnostic assays, and potentially therapeutic purposes.

Conflict of Interest

The Authors declare that they have no conflict of interests.

Acknowledgements

Supported by Key Projects of Quanzhou City (No. 2018Z017), International S&T Cooperation Program of China (No. 2016YFE0101700), State Key Laboratory of Cell Biology (No. SKLCB2018KF002), Project of Fujian Postgraduate Supervisor Team.

References

1) Cai J, Qi Q, Qian X, Han J, Zhu X, Zhang Q, Xia R. PD-1/PD-L1 axis regulation in cancer therapy. J Cancer Res Clin Oncol 2019; 145: 1377-1385.
2) Abbott M, Ustoyev Y. Cancer and the immune system: the history and background of immunotherapy. Semin Oncol Nurs 2019; 35: 1-5.
3) Zak KM, Grudnik P, Guzik K, Zieba BJ, Musielak B, Dömling A, Dubin G, Holak TA. Structural basis for small molecule targeting of the programmed death ligand 1 (PD-L1). Oncotarget 2016; 7: 30323-30335.
4) Huang X, Venet F, Wang YL, Lepape A, Yuan Z, Chen Y, Swan R, Kherouf H, Monneret G, Chung CS, Ayala A. PD-1 expression by macrophages plays a pathologic role in altering microbial clearance and the innate inflammatory response to sepsis. Proc Natl Acad Sci USA 2009; 106: 6303-6308.
5) Lim TS, Chew V, Sieow JL, Goh S, Yeong JPS, Soon AL, Castagnoli PR. PD-1 expression on dendritic cells suppresses CD8+T cell function and antitumor immunity. Oncoimmunology 2016; 5: 1085146-1085154.
6) Taube JM, Klein A, Brahmer JR, Xu H, Pan X, Kim JH, Chen L, Pardoll DM, Topalian SL, Anders RA. Association of PD-1, PD-1 ligands, and other features of the tumor immune microenvironment with response to anti-PD-1 therapy. Clin Cancer Res 2014; 20: 5064-5074.
7) Sharpe AH, Pauken KE. The diverse functions of the PD1 inhibitory pathway. Nat Rev Immunol 2018; 18: 153-167.
8) Ribas A. Adaptive immune resistance: how cancer protects from immune attack. Cancer Discov. Cancer Discov 2015; 5: 915-919.
9) Iwai Y, Ishida M, Tanaka Y, Okazaki T, Honjo T, Minato N. Involvement of PDL1 on tumor cells in the escape from host immune system and tumor immunotherapy by PD-L1 blockade. PNAS 2002; 99: 12293-12297.
10) Fang X, Tan W. Aptamers generated from cell-SELEX for molecular medicine: a chemical biology approach. Acc Chem Res 2010; 43: 48-57.
11) Tian H, Duan N, Wu S, Wang Z. Selection and application of ssDNA aptamers against spermine based on Capture-SELEX. Anal Chim Acta 2019; 1081: 168-175.
12) He J, Wang J, Zhang N, Shen L, Wang L, Xiao X, Wang Y, Bing T, Liu X, Li S, Shangguan D. In vitro selection of DNA aptamers recognizing drug-resistant ovarian cancer by cell-SELEX. Talanta 2019; 194: 437-445.
13) Liu KC, Lin BS, Lan XP. Aptamers: a promising tool for cancer imaging, diagnosis, and therapy. J Cell Biochem 2013; 114: 250-255.
14) Li F, Li Q, Zuo X, Fan C. DNA framework-engineered electrochemical biosensors. Sci China Life Sci 2020; 63: 1130-1141.
15) Guzik K, Zak KM, Grudnik P, Magiera K, Musielak B, Törner R, Skalniak L, Dömling A, Dubin G, Holak TA. Small-molecule inhibitors of the programmed cell death-1/programmed death-ligand 1 (PD-1/PD-L1) interaction via transiently induced protein states and dimerization of PD-L1. J Med Chem 2017; 60: 5857-5867.
16) Schägger H. Tricine-SDS-PAGE. Nat Protoc 2006; 1: 16-22.
17) Zak KM, Kitel R, Przetocka S, Golik P, Guzik K, Musielak B, Dömling A, Dubin G, Holak TA. Structure of the complex of human programmed death1, PD-1, and its ligand PD-L1. Structure 2015; 23: 2341-2348.
18) Setordzi P, Chang X, Liu Z, Wu YL, Zuo DY. The recent advances of PD-1 and PD-L1 checkpoint signaling inhibition for breast cancer immunotherapy. Eur J Pharmacol 2021; 895: 1-14.
19) Duan N, Gong WH, Wu SJ, Wang ZP. An ssDNA library immobilized SELEX technique for selection of an aptamer against ractopamine. Anal Chim Acta 2017; 961: 100-105.
20) Yazdian-Robati R, Arab A, Ramezani M, Abnous K, Taghdisi SM. Application of aptamers in treatment and diagnosis of leukemia. Int J Pharm 2017; 529: 44-54.